Meteoritics & Planetary Science 39, Nr 9, 1449–1460 (2004)
Abstract available online at http://meteoritics.org

SUPRACENTER: Locating fireball terminal bursts in the atmosphere using seismic arrivals

W. N. EDWARDS*† and A. R. HILDEBRAND

Department of Geology and Geophysics, University of Calgary, 2500 University Drive N.W., Calgary, Alberta, T2N 1N4, Canada
†Present address: Department of Earth Sciences, University of Western Ontario, Biological and Geological Sciences Building, London, Ontario N6A 5B7, Canada
*Corresponding author. E-mail: edwards@astro.uwo.ca

(Received 1 October 2003; revision accepted 17 July 2004)

Abstract–Terminal bursts and fragmentations of meteoritic fireballs in the atmosphere may now be accurately located in four dimensions (three spatial + temporal) using seismic arrival times of their acoustic waves recorded by seismometer, camera, microphone, and/or infrasound stations on the ground. A computer program, SUPRACENTER, calculates travel times by ray tracing through realistic atmospheres (that include winds) and locates source positions by minimization of travel time residuals. This is analogous to earthquake hypocenter location in the solid Earth but is done through a variably moving medium. Inclusion of realistic atmospheric ray tracing has removed the need for the simplifying assumption of an isotropic atmosphere or an approximation to account for "wind drift." This "drift" is on the order of several km when strong, unidirectional winds are present in the atmosphere at the time of a fireball's occurrence. SUPRACENTER-derived locations of three seismically recorded fireballs: 1) the October 9, 1997 El Paso superbolide; 2) the January 25, 1989 Mt. Adams fireball; and 3) the May 6, 2000 Morávka fireball (with its associated meteorite fall), are consistent with (and, probably, an improvement upon) the locations derived from eyewitness, photographic, and video observations from the respective individual events. If direct acoustic seismic arrivals can be quickly identified for a fireball event, terminal burst locations (and, potentially, trajectory geometry and velocity information) can be quickly derived, aiding any meteorite recovery efforts during the early days after the fall. Potentially, seismic records may yield enough trajectory information to assist in the derivation of orbits for entering projectiles.

INTRODUCTION

As asteroidal and cometary fragments enter the Earth's atmosphere, their extreme velocities cause sufficient frictional heating with the surrounding air to produce a plasma around the fragment body, thus forming the familiar fireball phenomena seen by observers on the ground. In addition, fireballs are capable of producing several different varieties of audible and sub-audible sound during their descent through the atmosphere, which have been recorded by ground-based instruments. These sounds can include audible booms and rumbling (~20–100 Hz) at the Earth's surface in the immediate area surrounding the fireball (up to ~200 km from the fireball's ground track depending on the source's altitude), which are produced by sonic booms created by the meteor's hypersonic travel, or explosive fragmentation/ disruption of the projectile (e.g., ReVelle 1975). At greater distances (several 100s to 1000s of km), audible frequencies have attenuated, leaving sounds to travel as sub-audible infrasonic sound (0.1–10 Hz) that may also be recorded by microbarometers or microbarometer arrays such as those reported by Brown et al. (2002) for two large bolides. Finally, electrophonic sounds may also be heard simultaneously with the visual fireball, caused by ELF/VLF radiation (radio waves) produced in some large fireballs' plasma and made audible by commonplace objects acting as transducers (Keay 1992). All of these sounds can provide information that is characteristic of the fireball source. Of particular interest to some researchers is how sound recordings on the ground can be used to locate the fireball sources and to constrain projectile kinetic energies.

As meteoroids in the 0.1–10 m-diameter range penetrate into the denser layers of the atmosphere, increasing pressures often cause the projectiles to fracture violently, either as a series of fragmentations or in a single explosive event termed a "terminal burst." Acoustic waves produced by these

explosions propagate to the ground and can be recorded by nearby seismometers (e.g., Qamar 1995) or by the ever more common security camera systems that may record sound in addition to video. If enough adequately separated stations record the same event, it becomes possible to locate the four-dimensional position (three spatial + time) of the explosion, or "supracenter," using computed travel times of the acoustic waves through the atmosphere. This process is analogous to the procedure used to locate earthquakes in the solid Earth yet is complicated by the anisotropic effects of atmospheric winds and the greater inhomogeneity of the atmosphere.

These explosive events are of particular importance to fireball investigation as they represent positions typically near the end of the visible and supersonic flight of a bolide. Accurately locating a bolide's terminal burst constrains meteorite strewn field predictions, while trajectory determination from a sequence of bursts may be sufficient to outline a strewn field. Either case will assist any meteorite recovery efforts that may follow.

THE SUPRACENTER PROGRAM

A supracenter is hereby defined as the location in space at a specific time of an explosive event located in the atmosphere. SUPRACENTER is a computer program that has been designed to locate the positions of atmospheric explosions using arrival times of their acoustic waves as recorded by instruments like seismometers on the ground, while incorporating realistic atmospheres. The procedure incorporates the methodology of locating earthquakes in the solid earth with the addition of ray propagation through an anisotropically moving, inhomogeneous medium.

This is not the first attempt to locate atmospheric sources related to explosive events like bolides; others have obtained solutions using atmospherically transmitted sound (e.g., Johnston 1987; Cumming 1989; Qamar 1995; Borovička and Kalenda 2002). However, all have assumed a static, isotropic atmosphere to simplify the ray tracing. In contrast, SUPRACENTER computes the true three-dimensional ray paths to each observing station, using realistic atmospheres that include the variability of temperature and wind as a function of altitude, by incorporating user-defined atmospheres derived from radiosonde and/or modelled data.

Supracenter Location

To locate the position of a supracenter, SUPRACENTER uses the procedure outlined by Nelson and Vidale (1990) for their QUAKE3D hypocenter location program. This method uses computed travel times to calculate an average time of occurrence, $\overline{T}$, for any event location via:

$$\overline{T} = \frac{1}{N}\sum^{N}(T_{obs} - T_{calc}) \quad (1)$$

where N is the number of seismic stations, T_{obs} are the observed arrival times, and T_{calc} are the computed travel times. This time is then used to evaluate individual travel time residuals for each seismic station and an M-estimate, R, of the error in position using an L2 residual method (Anderson 1982):

$$R = \frac{1}{N}\sum^{N}(T_{obs} - T_{calc} - \overline{T})^2 \quad (2)$$

As an alternative to this method, the median time of occurrence may be calculated instead of the mean, and the individual station residuals and M-estimate may be found using the L1 residual method (Nelson and Vidale 1990):

$$R = \frac{1}{N}\sum^{N}\left|T_{obs} - T_{calc} - \overline{T}\right| \quad (3)$$

In cases where seismic data of a terminal burst or fragmentation can be supplemented by a known occurrence time from video or satellite-derived light curves, the calculated time, $\overline{T}$, is replaced by the known time, T_k.

In all three instances, by minimizing the M-estimate value, R, over the volume of space encompassing the suspected source event, the position of the source (i.e., terminal burst) can be located.

SUPRACENTER has two options: automated and manual searches. The automated search uses a genetic search algorithm (Sambridge and Gallagher 1993) to efficiently search a volume of space designated by the user for the source position. The manual search allows the user to input the coordinates of individual test supracenters and interactively, through the use of residual maps and values, locate the position of the source.

DETERMINING RAY PATHS AND TRAVEL TIMES IN THE ATMOSPHERE

Before the calculation of travel times and ray paths, the fragmentation or terminal explosion in question is assumed to be a stationary point source explosion. Though bolide fragmentations occur during rapid travel through the atmosphere (i.e., a moving point source), durations of the explosions are typically very brief (<<1 sec), such that the produced sounds will still propagate outward quasi-spherically. Additionally, terminal explosions have been observed to produce spherical dust clouds (e.g., Hildebrand et al. 1999), so a stationary point source is still a good approximation. From here, the process of computing travel times from a given position of the point source to any given receiver position in SUPRACENTER is simplified further by only including those rays that travel directly from the source to the ground without turning (termed "direct arrivals"). This choice of direct arrivals, however, does not include Rayleigh

waves (or ground roll) that also are commonly recorded by seismometers from fireballs, even though both may occur in a seismic record. Though this restriction to direct arrivals places a limit on the most distant seismic observations that may be employed in a solution (typically, usable stations are restricted to within 100 km of the event epicenter), it allows use of a rapid method to obtain ray paths to a station. This method uses what is here termed a "ray net" that calculates the paths of multiple rays simultaneously while iteratively extending the optimal solution until a path is found that connects the source to the receiver.

To calculate individual ray paths, the generalized tau-spline or tau-p method of Garcés et al. (1998) for an inhomogeneous moving medium is used due to its relative adaptability to the ray net method. These equations are an extension of the original static tau-spline equations of Buland and Chapman (1983) for solid Earth models to rays propagating in the more fluid atmosphere and are essentially a high frequency, plane wave approximation to the actual wavefront. With broadband seismometers sensitive in the 0.01 to 50 Hz range, well above the lower limit of applicability estimated by Garcés et al. (1998), and minimal curvature of the wavefront at epicentral and greater ranges (departure of wavefront from a planewave at the surface is less than 2° for sources at altitudes of 20–40 km), the supracenter location meets the criteria necessary to apply the tau-p method.

Figure 1 illustrates the procedure used to construct the ray net for any given source and receiver pair. First, once the positions of the source and receiver have been specified, the height interval between the two points and the corresponding temperature and wind information are identified. This interval will be identical for all direct arrival rays. The ray net is then centered on the azimuth connecting the source and the receiver, and the azimuths ±90° from this direction are sampled every two degrees. For each of these chosen azimuths, a series of takeoff angles ranging from 90° to 180° from the vertical are then sampled, at the same two-degree interval, forming an equally spaced, quarter hemispherical, 73 × 37 grid of potential ray propagation directions (Fig. 1a). This is the initial form of the ray net.

For each azimuth/takeoff angle pair in the ray net, the wind components parallel and perpendicular in each layer of the height interval are found, and their corresponding ray parameters are calculated via:

$$p = \frac{\alpha}{c}\left(1 + \alpha\frac{u}{c}\right)^{-1} \quad (4)$$

where α is the wave front normal direction cosine for the x-direction, c is the ambient sound speed, and u is the component of the wind vector along the chosen azimuth. Each individual ray path is then calculated for all the azimuth/takeoff angle pairs simultaneously over the altitude interval for direct arrivals (containing i individual stratified layers) using:

$$\Delta X_j = \sum_i \left(\frac{p_j}{(1 - p_j u_i)} + s_i^2 u_i\right)\left(s_i^2 - \frac{p_j^2}{(1 - p_j u_i)^2}\right)^{-1/2} \Delta z_i \quad (5)$$

$$\Delta Y_j = \sum_i (s_i^2 v_i)\left(s_i^2 - \frac{p_j^2}{(1 - p_j u_i)^2}\right)^{-1/2} \Delta z_i \quad (6)$$

(Garcés et al. 1998) and Matlab's vector-based computation abilities. Here, $s_i = 1/c_i$, while u_i and v_i are the wind components, parallel and perpendicular, respectively, to the chosen azimuth associated with the value of the ray parameter, p_j, for the ith layer in the interval with a thickness of $\Delta z_i = | z_i - z_{i+1} |$.

Final destination coordinates for each of the azimuth/takeoff pairs are then found and compared to the receiver position. Next, the azimuth/takeoff pair that is closest to the receiver is chosen as the center for the next iteration of the ray net (position P in Figs. 1a and 1b). The eight surrounding points of this minimum define the boundaries for a new, equally spaced 37 × 37 grid of azimuth/takeoff pairs, now with a spacing of 0.055°. Parallel and perpendicular wind components are then recalculated for each azimuth/takeoff pair in the new grid and are then ray traced and compared again with the receiver position. Third, if necessary, the grid is again expanded about the minimum (position P2 in Figs. 1b and 1c) for the next iteration and so on until a path is found that reaches the receiver. Acceptance of a particular ray path is made when the ray reaches to within 1 km of the receiver position. Failure to find such a path results in a similar search for rays passing within 1 km over the receiver. Should the search fail again to find a path, the search is terminated for that receiver with the conclusion that no direct arrival path to that receiver is possible. If a path is found that connects the source and receiver, a travel time is then calculated for the connecting azimuth/takeoff pair using (Garcés et al. 1998):

$$\Delta T_{ij} = s_i^2\left(s_i^2 - \frac{p_j^2}{(1 - p_j u_i)^2}\right)^{-1/2} \Delta z_i \quad (7)$$

TRAVEL TIME ERROR

The error in computed travel time using the ray net method was explored using several windy isotropic models. These simplistic atmospheric models, equivalent to the individual layers of a more complex stratified atmosphere, allowed the computed ray net travel times to be directly compared with their analytic counterparts. Using a 126 × 126 grid sampling an area of 200 km^2, rays and travel times were calculated to all points in the grid, both analytically and via the ray net method, from a source located at the center of the grid at various altitudes. The two travel times were then

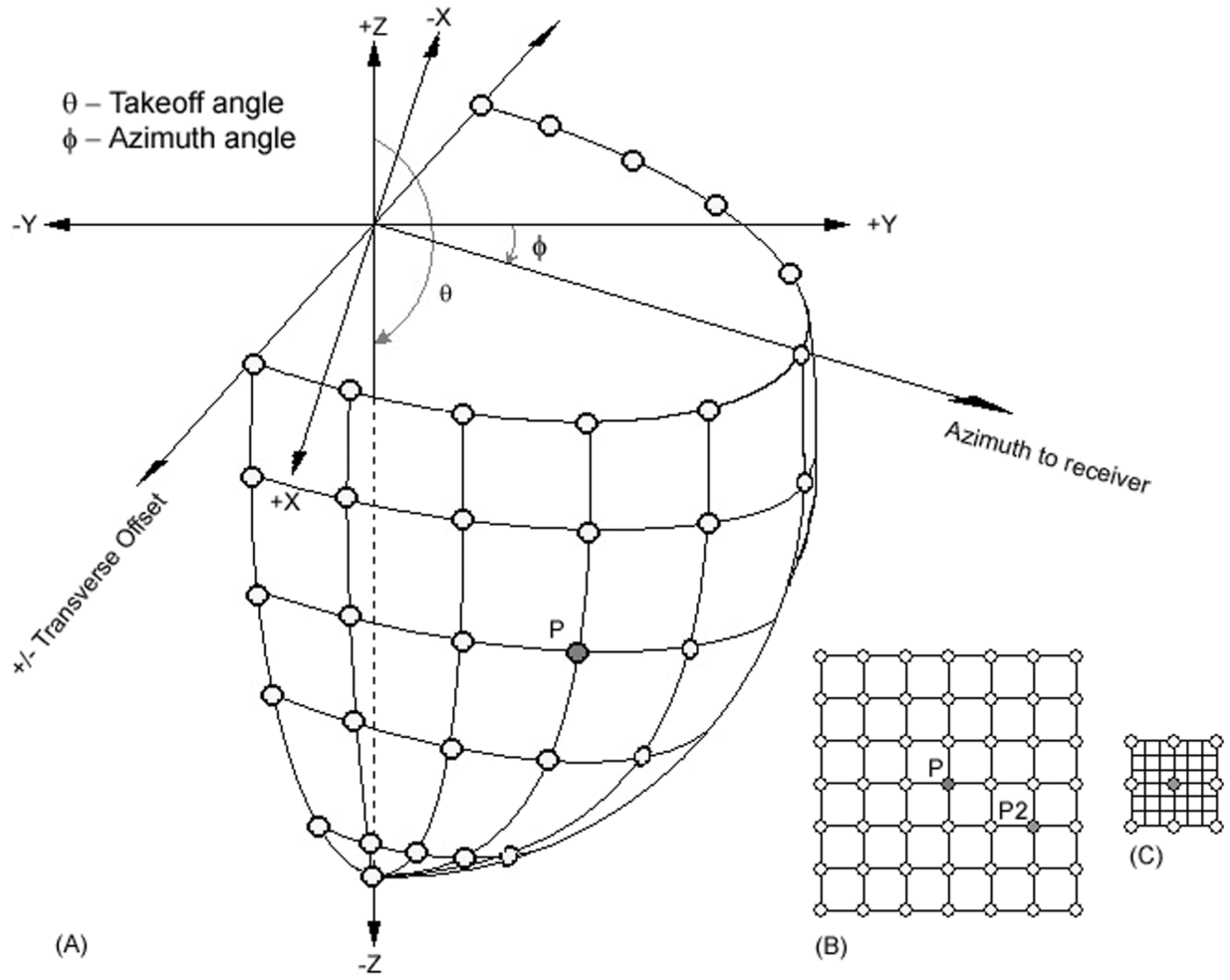

Fig. 1. A schematic diagram of the ray net expansion: a) the ray as constructed at the beginning of the refinement procedure; b) the azimuth/takeoff pair (P) is closest to the receiver, thus, pair P and its surrounding pairs are refined to a smaller sampling; c) the procedure is repeated for the new closest pair (P2) and so on until the ray path to the receiver is found or refinement of the ray net is terminated.

compared with the error, expressed as a percentage of the total analytical travel time.

Through the mapping of this percentage error in travel time, areas of excessive systematic error could not be found. Errors in calculated travel time are random, likely corresponding to missing the target position by a few meters, yet are symmetric about the direction of the wind (an example of a percentage error map is shown in Fig. 2). When wind magnitudes were varied from 5 m/s to 90 m/s, representing 5% to 30% of the ambient sound speed and covering the maximum range of winds expected in the lower stratosphere and troposphere, percentage errors in travel time typically did not exceed 0.05% (positive or negative), corresponding to a total travel time error range of –0.049 to 0.0018 sec (Table 1). In nearly all trials, the largest of these errors occurred in the area vertically below the source.

Since the SUPRACENTER calculation method produces travel time errors of hundredths of seconds along a ray path that may propagate for many minutes, the errors in calculated travel time can be considered to be negligible in comparison to the approximations and assumptions used when reconstructing the ambient atmospheres for fireballs. The reader should also be aware that a variety of anomalous ray propagation effects may occur in the real atmosphere (see ReVelle [1974, 1976] for a discussion of these effects).

Table 1. Maximum and minimum travel time and percentage error for various wind magnitudes using the ray net method.

	Percentage error (%)		Travel time error (sec)	
Wind speed[a]	Maximum	Minimum	Maximum	Minimum
5.0	0.0015	–0.0015	0.0033	–0.0033
10.0	0.0017	–0.046	0.0035	–0.046
15.0	0.0018	–0.0049	0.0038	–0.0049
20.0	0.0017	–0.033	0.0039	–0.034
25.0	0.0016	–0.032	0.0041	–0.033
30.0	0.0017	–0.048	0.0046	–0.049

[a]Percent of ambient sound speed.

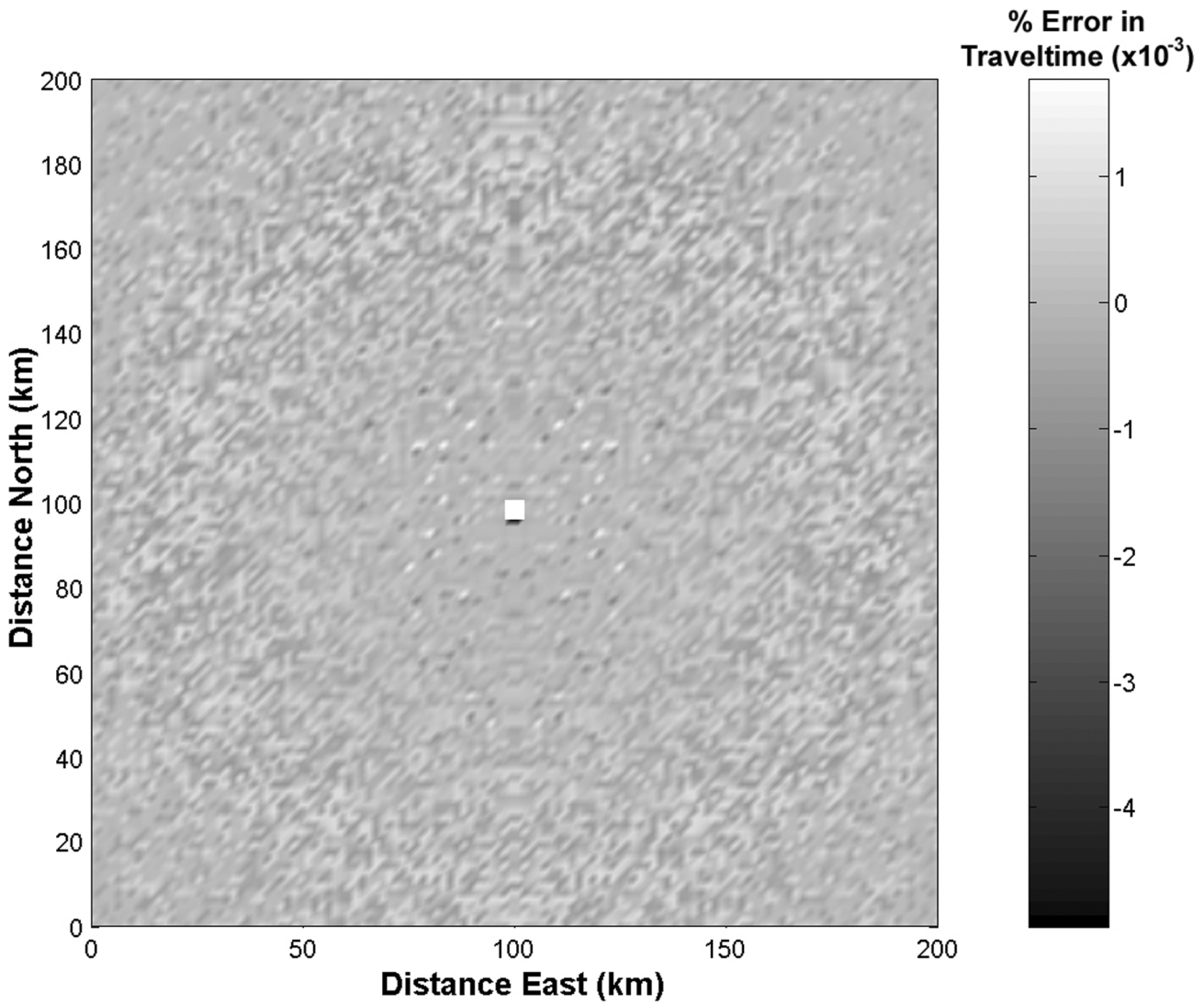

Fig. 2. An example of a percentage error map in total travel time to a 200 km^2 area from a central 30 km altitude source in a windy, isotropic atmosphere. The ambient sound speed is 300 m/s with winds of 45 m/s from the north.

CASE STUDIES

SUPRACENTER's ability to locate meteor terminal bursts and fragmentation events along a fireball's trajectory may be tested using several fireball events where observational and/or photographic records are available along with seismic data.

El Paso Superbolide

On October 9, 1997, during the local noon hour, a bright fireball exploded near the city of El Paso, Texas, USA. Witnesses saw the fireball and captured its dust clouds in photographs and on video. The energy released by the terminal burst was determined to be equivalent to ~0.5 kt of TNT, based on satellite observations of the amount of visible light emitted (Wacker et al. 1998; U.S. Air Force 1997), producing a circular shock around the detonation with a radius of ~500 m. The acoustic waves produced by the terminal burst were of sufficient strength to be recorded by seven separate seismic stations, with the most distant station being 239 km away from the first acoustic recording. The earliest acoustic arrival had been recorded by a local security camera's record of a witness reacting to the sound's arrival. Hildebrand et al. (1999) triangulated the position of the bolide's terminal burst, using handheld compass-measured azimuths and altitudes from photographs and video of the fireball's dust cloud taken at early times (between 2 and 3 min) after the bolide's passage. The positions of the eyewitness photographers were reconstructed, and dust cloud bearings were taken relative to the foreground objects. The derived position was 31.80°N, 106.06°W. The altitude of ~28.5 km (Hildebrand et al. 1999) was derived using an assumed velocity of 305 m/s for

the MUD security arrival. In addition, the El Paso bolide was located by optical/infrared sensors on board U.S. Department of Defense (DoD) satellites, which placed the terminal explosion at 31.8°N, 106.1°W at an altitude of 36 km (U. S. Air Force 1997).

SUPRACENTER was able to determine a new location for the terminal burst using: 1) the arrival times from the two nearest seismic stations (determined in the initial investigation from records obtained from the Kidd Seismological Observatory at the University of Texas, El Paso); 2) the arrival time identified on the security camera recording; 3) the DoD satellite-observed time of the terminal burst (18:47:15 UT); and 4) a realistic atmospheric model derived from a radiosonde released from the El Paso International Airport (31.804°N, 106.373°W, 1206 m a.s.l.) before (11:00:00 UT) the fireball's descent (Fig. 3). The new location lies ~2.1 km west-southwest upwind of the position determined by Hildebrand et al. (1999) at 31.790°N, 106.080°W, and 27.6 km a.s.l. (Fig. 4). However, this new location excludes the ~500 m of non-linear, supersonic travel of the initial shock that immediately surrounded the bolide's terminal explosion. The omission of this shock, due to the assumption that all waves will propagate at ambient acoustic speeds (in the absence of wind), will tend to provide solutions at slightly lower altitudes than would be expected had the initial shock been accounted for. After the inclusion of the shock, altitudes of the Hildebrand et al. (1999) and SUPRACENTER positions are in good agreement within error. Additionally, the presence of a prominent wind shear at ~30 km altitude that rapidly distorted the bolide's dust cloud above the roughly circular cloud, produced by the terminal burst (as seen in photographs and video), confirms that the supracenter position must lie below this feature.

These same upper atmospheric winds would eventually distort and transport the bolide's dust trail between several hundred m and several km away from its original position during the 2–20 min time interval of the eyewitness photographs and video. This will introduce some measure of error in geographic positioning. Thus, SUPRACENTER's location for the terminal burst is probably better than that found through the analysis of photographs and video of the fireball's dust clouds. The projectile is thought to have been almost completely pulverized by the terminal burst due to the large entry velocity (~25 km/s; Hildebrand et al. 1999), the lack of sizable dust clouds at lower elevations, and the lack of meteorites found in the projected fall area.

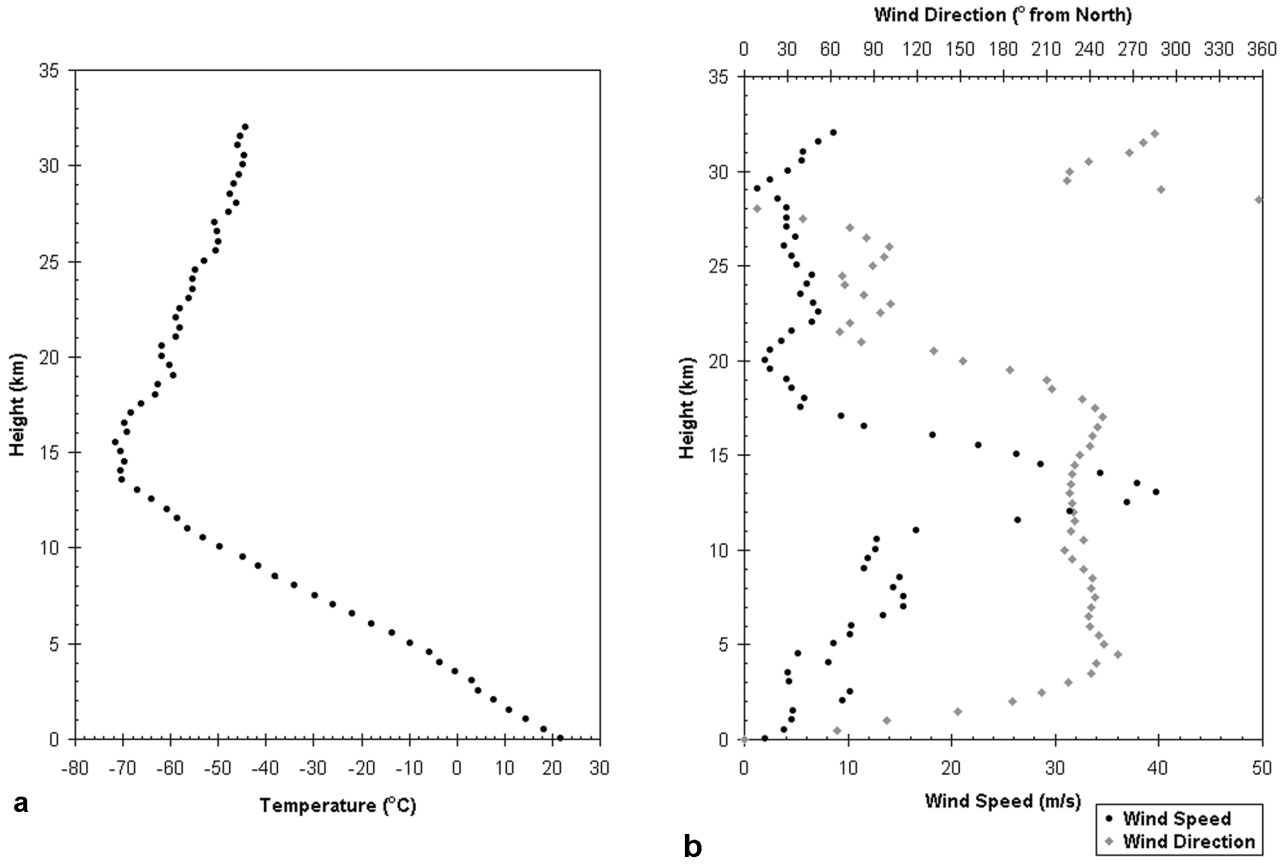

Fig. 3. Atmospheric models to 32 km altitude for the El Paso superbolide. Derived from the October 9, 1997 11:00:00 UT El Paso International Airport radiosonde release: a) temperature; b) wind speed and direction.

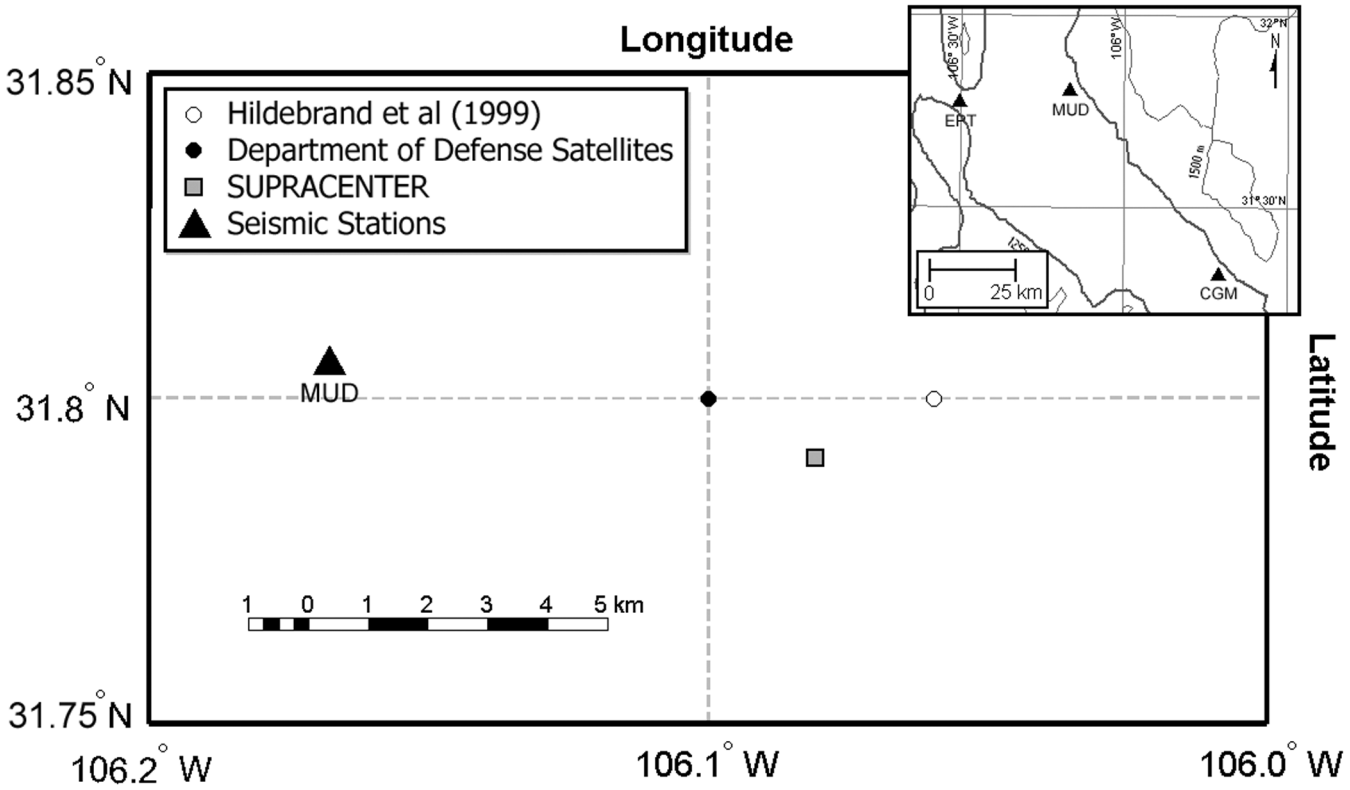

Fig. 4. A comparison map of the location reported by Hildebrand et al. (1999), the DoD satellite observed location, and that found by SUPRACENTER for the superbolide's terminal burst. Inset: the location of the nearest three seismic/acoustic detections is shown.

Mt. Adams Fireball

On January 25, 1989, during the local noon hour, witnesses in northwestern Washington observed a fireball traveling to the southwest. The fireball, after traveling some distance, was observed to split, forming two distinct tails (Scientific Event Alert Network 1989). Soon after this separation, one of the fireballs exploded, leaving the second to travel further downrange before it also exploded near the northwest flanks of Mount Adams (Pugh 1990). Though a search for surviving meteoric material was attempted, new snowfall caused searches to be suspended. Although these searches found nothing, the arrival of the acoustic waves produced by the terminal bursts were recorded by 26 seismic stations of the Pacific Northwest Seismic Network. The two distinct pulses of the individual explosions were identified (after having been initially dismissed as noise) once reports of the fireball were received. The low apparent velocity of the pulses indicated an atmospheric source upon re-examination (Qamar 1995).

Realizing that the source positions of these two explosions potentially could be found, Qamar (1995) used a static, isotropic atmosphere based on an average acoustic velocity to locate the events, assuming stationary point sources for the fireball's two terminal bursts. Fortunately, Qamar was foresightful and provided the arrival times for the two pulses for the 26 stations, which provided an opportunity to test SUPRACENTER with a well-observed twin explosion fireball.

To improve on Qamar's solutions, atmospheric data were needed to reproduce temperature and wind conditions present at the time of the fireball's descent. Historical radiosonde records were found for the days before, on, and after the fireball for the two nearest release points, Quillayute (47.950°N, 124.55°W, 56 m a.s.l.) to the west and Spokane (47.633°N, 117.53°W, 720 m a.s.l.) to the east. Though both releases were distant (326 km and 308 km from Mt. Adams, respectively), measured profiles for temperature and wind were similar for both stations both before and after the fireball. This, likely, is due to the typical stability of the atmosphere during the winter months. The Spokane sounding was chosen to represent the first 27 km of the atmosphere. However, no data existed in either sounding for greater altitudes. To extend the reconstructed atmosphere to greater heights, modelled data were used. Temperatures were extrapolated using the profile of the 1976 U.S. Standard Atmosphere (United States Committee on Extension to the Standard Atmosphere 1976), and wind speed and direction were found using the Naval Labs Horizontal Wind Model (Hedin et al. 1996). After interpolation between the two sources, an atmosphere was produced that is likely similar to that present in the Mt. Adams region at the time of the fireball's decent (Fig. 5).

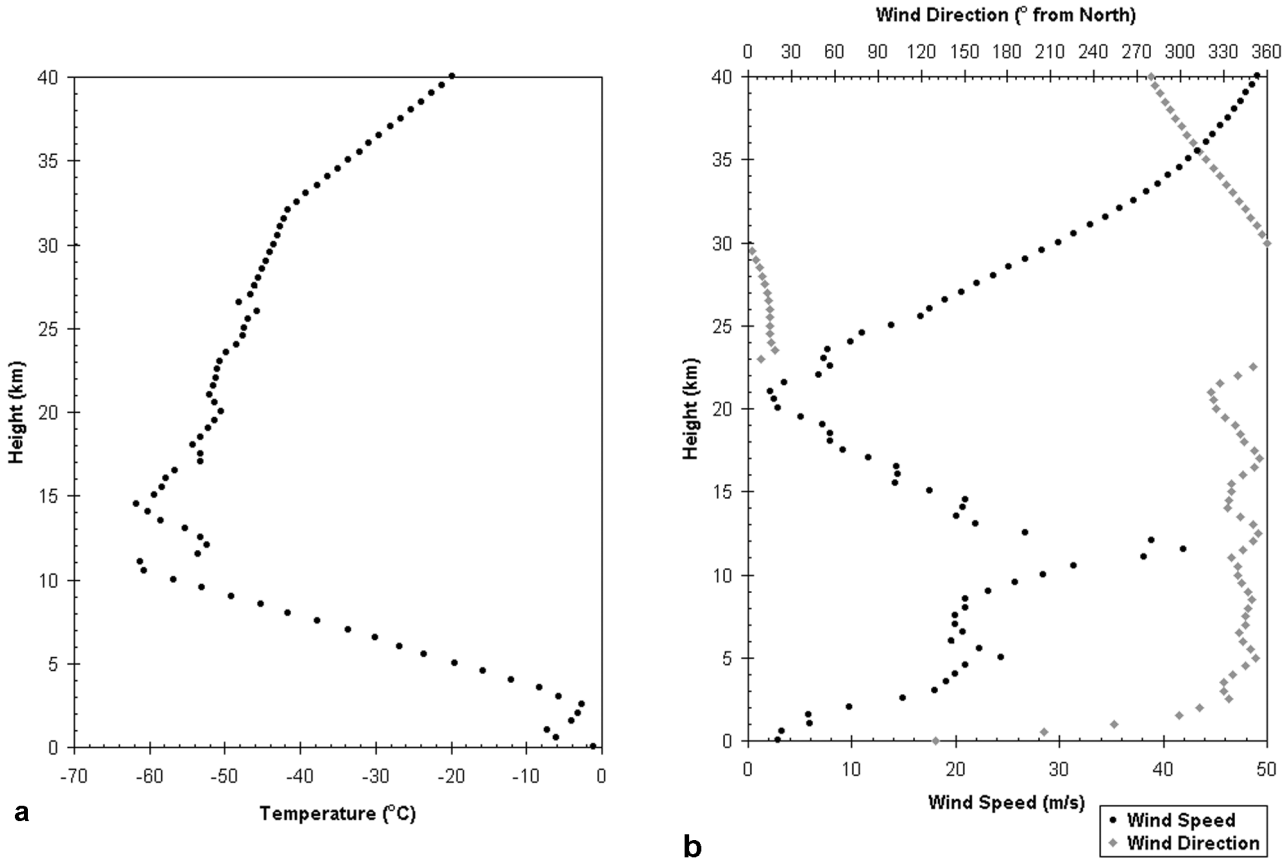

Fig. 5. Atmospheric models to 40 km altitude for the Mt. Adams fireball. Reconstructed from historical radiosonde data and the 1978 USSA and HWM models: a) temperature; b) wind speed and direction.

Using the reconstructed atmosphere and the arrival times reported by Qamar (1995), locations were found for the two fragmentation events near the end of the Mt. Adams fireball's luminous trajectory using SUPRACENTER. These two locations (A and B) lie at 46.460°N, 122.096°W, and 34.6 km a.s.l. and 46.418°N, 122.065°W, and 29.8 km a.s.l. at 20:51: 14.5 and 20:51:15.1 UT, respectively, and are ~2.7 and 2.5 km north-northwest (upwind) of those reported previously by Qamar (Fig. 6).

A comparison of the SUPRACENTER-derived solutions to the isotropic solutions of Qamar was performed using the station residual statistics. Since residuals were not given for Qamar's solutions, similar locations were obtained using an isotropic atmosphere with an acoustic velocity of 305 m/s. The statistics of the station residuals obtained from the isotropic atmosphere assumption were then compared with those found using the reconstructed atmosphere (Table 2). Though direct arrivals could only be found for 21 of the 26 stations (the remaining five for each burst were located at epicentral distances ranging between 42 and 71 km) with the reconstructed atmosphere, statistics of the residuals for the two atmospheric models were found to be similar but with a slight improvement with the reconstructed atmosphere, showing that both models can locate the two terminal bursts with nearly equal internal consistency. However, the reconstructed atmosphere solution demonstrates that the presence of strong unidirectional winds can have a considerable effect on the position of any supracenter solution. Including wind and temperature profiles that were present during the fall of the Mt. Adams fireball probably improves the positions found by Qamar (1995), and the results are likely closer to the true positions of the two terminal bursts.

Table 2. Residual statistics for the locations of the two terminal bursts for the Mt. Adams fireball using isotropic and reconstructed atmospheres.

	Isotropic atmosphere		Reconstructed atmosphere	
Terminal burst	A	B	A	B
Mean absolute residual	1.393	1.175	0.925	0.903
Standard deviation	1.939	1.672	1.230	1.489

In addition, the separation of the two bursts in space and time allow the azimuth, elevation angle, and approximate velocity of the fireball to be found. Using the values found by SUPRACENTER for terminal bursts A and B, an azimuth of 152°, elevation angle of 43°, and velocity of 11.7 km/s are found for the Mt. Adams fireball. These values are consistent

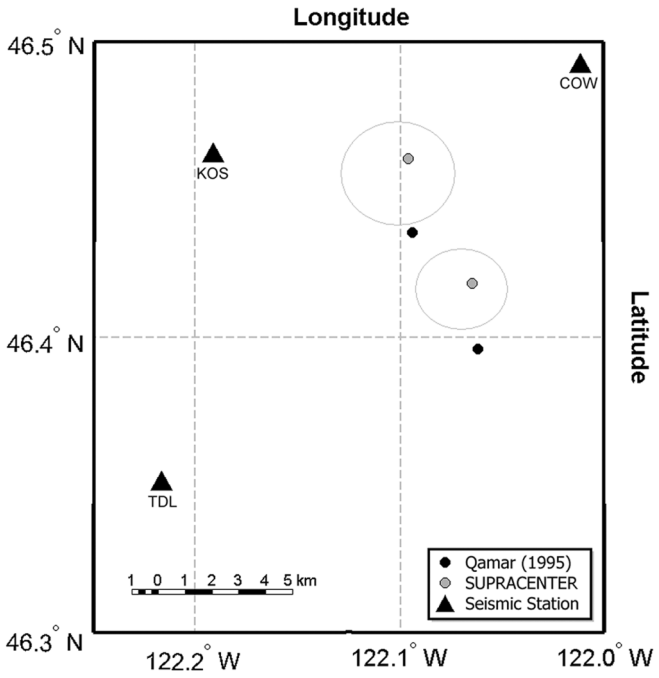

Fig. 6. A comparison map of the solution positions for the two Mt. Adams fireball terminal bursts found by SUPRACENTER and reported by Qamar (1995). The gray ellipses designate regions of a standard deviation increase in the mean absolute travel time residual for the SUPRACENTER locations.

with the fireball traveling from Puget Sound to the northwest flank of Mt. Adams, as reported by Pugh (1990), while the velocity of ~12 km/s lies near the low end of observed fireball velocities. Potentially, this velocity could be somewhat larger, as solutions using L1 and L2 methods give similar locations with intervals between burst times that differ on the order of ±0.3 sec. Since typical fireball velocities may traverse the distance between the two Mt. Adams terminal bursts in similar sub-second times, determination of the fireball velocity is poorly constrained by the seismic records in this case, as pointed out previously by Qamar (1995).

This velocity resolution problem of using seismic arrivals stems from the properties of meteors and sound propagation. Since meteors travel hypersonically (11.3–72.6 km/s) and sound waves travel significantly slower (~0.310 km/s) in the atmosphere, if fragmentations occur rapidly one after another (i.e., a fraction of a sec), sound waves produced from the first fragmentation have not travelled far when the following fragmentation occurs. As these waves propagate to the ground over the time scales of several to many minutes, the atmosphere effectively attenuates high frequency components of the wave and spreads out the wave energy through dispersion. Thus, when the wave is recorded by seismographs, a specific time of arrival may be a matter of interpretation, leading to an error in arrival time picks on the order of several tenths of seconds, the same magnitude (or larger) as the differences in occurrence time between bursts or fragmentations. In addition, the assumptions and approximations made during reconstruction of the atmospheric temperature and wind velocity structure (which determine the sound wave propagation speed) further contribute to timing and location uncertainties between fragmentations, as knowledge of the atmosphere often is obtained at a distance from the actual location of the bolide and at times that may be hours before or after the actual occurrence of the event. Therefore, accurately constraining a fireball's velocity is difficult and sometimes impracticable by seismic methods. In the specific case of the Mt. Adams fireball, no other instrumental records existed that allowed for more precise determination of the two terminal burst occurrence times or the time duration between them. Hence, the uncertainties in the two occurrence times and the fireball's velocity remain. We note that a video record of such fireball explosions, even if otherwise unreferenced, would provide the duration between the bursts, and given the time and locations obtained with SUPRACENTER, a reasonably valid fireball trajectory and velocity may be derived.

Morávka Fireball and Meteorite Fall

On May 6, 2000, a fireball was well-observed and recorded by several different instruments falling near the town of Morávka in the Czech Republic (Borovička et al. 2003a b; Brown et al. 2003; Borovička and Kalenda 2003). The variety and quality of video and other data allowed a determination of not only the initial fireball's trajectory (azimuth: 175.5°, elevation: 20.4°, velocity: 22.5 km/s) but also the bolide's pre-fall orbit. When meteorites were recovered near the town, this event became only the sixth meteorite fall in history to have a known pre-fall orbit.

Among the recovered data were seismic records from a series of stations (operated by local academic and industrial institutions) straddling the fireball's trajectory. From these records, Borovička and Kalenda (2003) identified acoustic arrivals from 12 individual fragmentation events along the fireball's trajectory. Using these arrival times and a static isotropic atmosphere simplified from the known temperature profile, locations for each of the fragmentations were found. An approximate correction for "wind drift" shifting these locations upwind was then applied. SUPRACENTER was employed to check the validity of the locations were found by Borovička and Kalenda for several fragmentations. Conditions at the time of the fireball of the lower atmosphere were known from radiosonde-measured temperature and winds and were supplemented by modelled data to produce a reconstructed atmosphere to an altitude of 200 km (Brown et al. 2003). Although arrival times to each station were not given explicitly, Borovička and Kalenda provided a figure in which they identified the relative positions of arrivals for six of the 12 fragmentations on 11 station records (fragmentations C, E, F, G, K, and L). These arrival times, along with the

atmospheric data, were input into SUPRACENTER, and supracenters found for these six fragmentations.

Though initial solution epicenters showed good agreement, occurrence times (and, hence, the fragmentation altitudes) showed significant variation on the order of 8 sec. As the fragmentations occurred rapidly and sequentially, event C first and L last, a second set of solutions was found after constraining all occurrence times to that recorded by Earth-observing satellites, 11:51:52.5 UT. With this new constraint, the heights of fragmentation events significantly improved, reducing the scatter along the known fireball trajectory. Overall station residuals were very low for each fragmentation supracenter (Table 3), and tolerable agreement existed between the solutions found by Borovička and Kalenda (2003) and SUPRACENTER, though the latter consistently lay south of the former (Fig. 7). This is thought to be due to the incorporation of a realistic wind model instead of the approximation used by Borovička and Kalenda. These differences were generally small, ranging between 0.4 and 0.8 km for most supracenters, well within atmospheric modelling error, although event K shifted ~1.5 km to the south-southwest. These new supracenters suggest a more easterly azimuth of 171.8° and a shallow elevation angle of 18.9° for the Morávka fireball than the video-derived values of 175.5° and 20.4° (Borovička et al. 2003a). This trajectory difference is similar to the findings of Borovička and Kalenda.

Viewing the new supracenters from the perspective of the Kunovice video allowed further comparison between isotropic and realistic models. Figure 8 shows that the SUPRACENTER positions for the fragmentations somewhat better align with the fireball trajectory/fragments recorded in

Table 3. Supracenter locations and associated residual statistics for six Morávka fireball fragmentations.

Event	Latitude (°N)	Longitude (°E)	Altitude (km a.s.l)	Mean abs residual (sec)	Residual σ (sec)
C	49.9728	18.4771	35.45	0.390	0.519
E	49.9431	18.4787	33.35	0.172	0.239
F	49.9221	18.4867	32.58	0.431	0.526
G	49.9141	18.4885	32.10	0.329	0.426
K	49.8625	18.4856	30.55	0.200	0.276
L	49.8052	18.5085	28.63	0.250	0.333

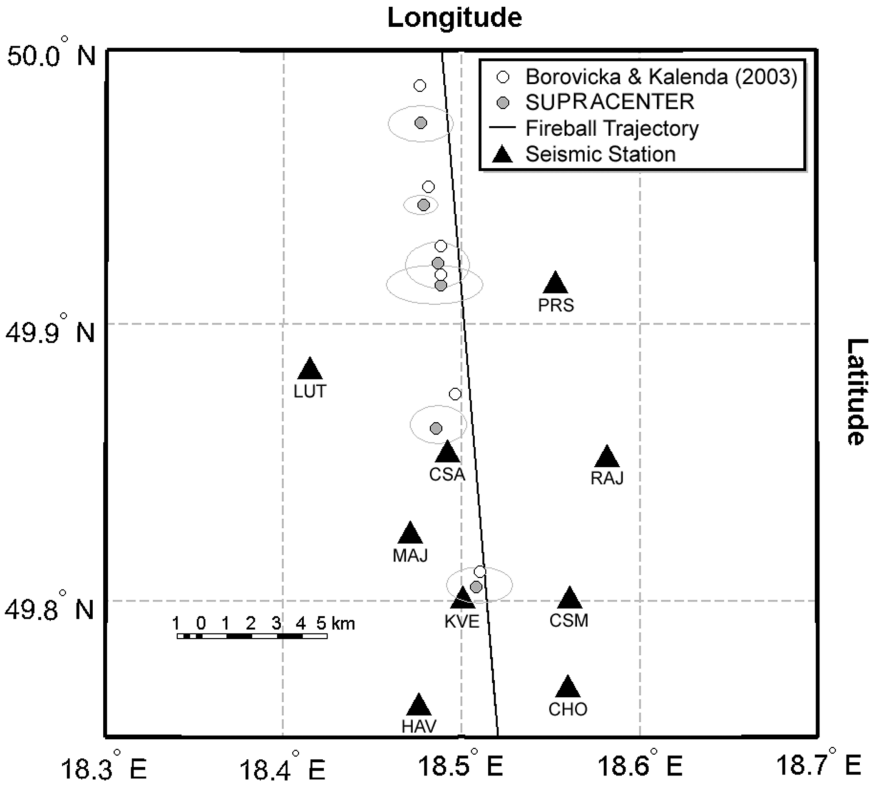

Fig. 7. A comparison map of six fragmentation event locations along the Morávka fireball trajectory as found by Borovička and Kalenda (2003) and SUPRACENTER. The gray ellipses designate regions of a standard deviation increase in the mean absolute travel time residual for the SUPRACENTER locations.

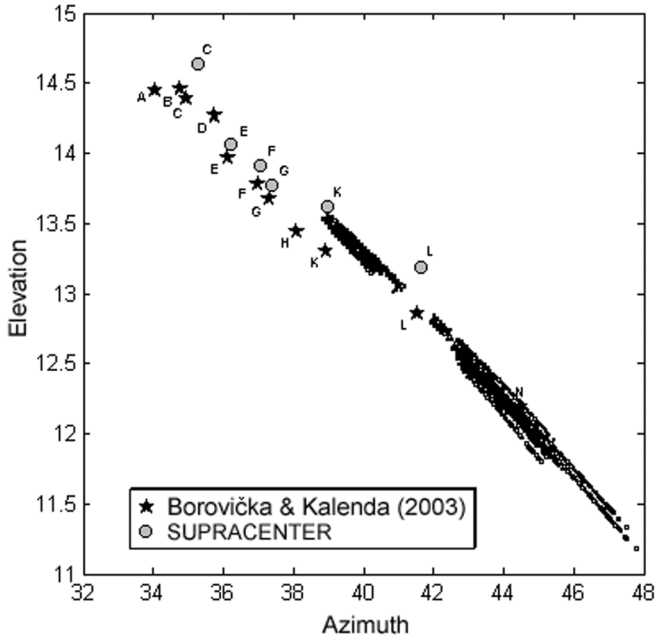

Fig. 8. Fragmentation event supracenters of Borovička and Kalenda (2003) and SUPRACENTER as seen from the Kunovice video perspective. The open squares represent individual fragments mapped from the Kunovice video.

the Kunovice video. For example, fragmentation K now lies near the beginning of a shower of fragments. Of particular interest is event L, which lies some distance above the observed shower of fragments. This is likely due to event L occurring later than the imposed occurrence time. To correct this, event L's altitude was lowered until its azimuth matched that of the beginning of the fragmentation shower (~13°), while its occurrence time was allowed to vary. This altitude difference was only 300 m, with the occurrence time increasing to 11:51:53.41 UT and the average absolute station residual increasing slightly to 0.275 sec. If this new occurrence time is taken to be accurate for event L, and the previous time of 11:51:52.5 UT is taken as the occurrence time of event C, a velocity of 22.1 km/s is found for the fireball. This is in excellent agreement with the velocity of 22.5 km/s found by Borovička et al. (2003a) for the fireball using video analysis. We also note the potential to compare the geometry of specific fragmentation events to the timing provided by the satellite-derived light curve fragmentation record, if a complete ground based light curve for the Morávka fireball had been observed.

DISCUSSION AND CONCLUSIONS

We have designed and constructed a supracenter location program to locate point source explosions in the atmosphere in four dimensions using recorded times of direct arrival acoustic waves. To our knowledge, it is the first of its kind to incorporate ray tracing through realistic atmospheres that include the anisotropic effects of wind to account for "wind drift." This is a significant departure from earlier isotropic assumptions used by previous authors. The consistencies with various other methods of fireball investigation demonstrate SUPRACENTER's utility.

The testing of the SUPRACENTER program with three recent and historical seismically recorded fireball events has produced results that are consistent with eyewitness, photographic, and video observations obtained during the initial fireball investigations and demonstrate that supracenter location is a viable method for locating fireball terminal bursts and/or individual fragmentation events. In cases where several individual bursts or fragmentation events are present for a fireball, trajectory and velocity information can also be found with some measure of accuracy. Most importantly, it has been shown that, when in the presence of strong unidirectional winds, the apparent wind drift for an individual supracenter can be on the order of 2–3 km. Position drifts of this size are significant as many known meteorite strewn field widths are of similar scale and, depending on the orientation of a fireball's trajectory, this may shift search areas significantly. The ease and rapidity of deriving fireball trajectory locations once seismic data are available means that meteorite recovery efforts can be better targeted during the early days of an investigation.

In addition, other sources of data such as light curves, flashes, and direct observations recorded by satellites, photographs, or video can provide important constraints on the exact time of occurrence, spacing, and position for individual supracenters. These uniquely constrain the supracenter(s), and these sources should be exploited whenever available to improve location solutions.

Though we have used this program specifically for use in locating fireball terminal bursts, it conceivably can be used for any kind of explosive point sources located in the atmosphere.

Future work on supracenter location will be focused on the inclusion of stratospheric and thermospheric returns (detected by distant seismic or infrasound arrays) to the solution. This should extend the usefulness of the technique to events where direct arrivals are few or non-existent yet where distant observations are more plentiful.

Acknowledgments–Thanks go out to Peter Brown for his discussions on acoustic wave arrivals, timely model atmosphere calculations, access to the findings and data of the Morávka meteorite fall investigation, and feedback during the development of this program. To the National Oceanic and Atmospheric Administration (NOAA) and the CARDS radiosonde database for historical upper atmosphere data, and finally, to the anonymous reviewer for pointing out potential future problems incorporating stratospheric returns with our current method and for helpful comments.

Editorial Handling—Dr. Donald Brownlee

REFERENCES

Anderson K. R. 1982. Robust earthquake location using M-estimates. *Physics of the Earth and Planetary Interiors* 30:119–130.

Borovička J., Spurny P., Kalenda P., and Tagliaferri E. 2003a. The Morávka meteorite fall: 1. Description of the events and determination of the fireball trajectory and orbit from video records. *Meteoritics & Planetary Science* 38:975–987.

Borovička J., Weber H. W., Jopek T., Jakeš P., Randa Z., Brown P. G., Revelle D. O., Kalenda P., Schultz L., Kucera J., Haloda J., Tycová P., Fryda J., and Brandstätter F. 2003b. The Morávka meteorite fall: 3. Meteoroid initial size, history, structure, and composition. *Meteoritics & Planetary Science* 38:1005–1021.

Borovička J. and Kalenda P. 2003. The Morávka meteorite fall: 4. Meteoroid dynamics and fragmentation in the atmosphere. *Meteoritics & Planetary Science* 38:1023–1043.

Brown P., Whitaker W., Revelle D., and Tagliaferri E. 2002. Multi-station infrasonic observations of two large bolides: Signal interpretation and implications for monitoring of atmospheric explosions. *Geophysical Research Letters* 29:1–4.

Brown P., Kalenda P., Revelle D., and Borovička J. 2003. The Morávka meteorite fall: 2. Interpretation of infrasonic and seismic data. *Meteoritics & Planetary Science* 38:989–1003.

Buland R. and Chapman C. H. 1983. The computation of seismic travel times. *Bulletin of the Seismological Society of America* 73: 1271–1302.

Cumming L. G. 1989. Alberta bolide of June 1, 1982: Interpretation of photographic and seismic records. *Canadian Journal of Earth Science* 26:1350–1355.

Garcés M. A., Hansen R. A., and Lindquist K. G. 1998. Travel times for infrasonic waves propagating in a stratified atmosphere. *Geophysical Journal International* 135:255–263.

Hedin A. E., Fleming E. L., Manson A. H., Schmidlin F. J., Avery S. K., Clark R. R., Franke S. J., Fraser G. J., Tsuda T., Vial F., and Vincent R. A. 1996. Empirical wind model for the upper, middle, and lower atmosphere. *Journal of Atmospheric and Terrestrial Physics* 58:1421–1447.

Hildebrand A. R., Brown P., Crawford D., Boslough M., Chael E., Revelle D., Doser D., Tagliaferri E., Rathbun D., Cooke D., Adcock C., and Karner J. 1999. The El Paso superbolide of October 9, 1997 (abstract #1525). 30th Lunar and Planetary Science Conference. CD-ROM.

Johnston A. C. 1987. Airblast recognition and location using regional seismographic networks. *Bulletin of the Seismological Society of America* 77:1446–1456.

Keay C. 1992. Electrophonic sounds from large meteor fireballs. *Meteoritics* 27:144–148.

Nelson G. and Vidale J. 1990. Earthquake locations by 3-D finite-difference travel times. *Bulletin of the Seismological Society of America* 80:395–410.

Pugh R. N. 1990. The Mt. Adams, Washington fireball of January 25, 1989 (abstract). *Meteoritics* 25:400.

Qamar A. 1995. Space shuttle and meteoroid: Tracking supersonic objects in the atmosphere with seismographs. *Seismological Research Letters* 66:6–12.

Revelle D. G. 1974. Acoustics of meteors: Effects of the atmospheric temperature and wind structure on the sounds produced by meteors. Ph.D. Thesis, University of Michigan, Ann Arbor, Michigan, USA.

Revelle D. G. 1975. Studies of sounds from meteors. *Sky and Telescope* 2:87–91.

Revelle D. G. 1976. On meteor-generated infrasound. *Journal of Geophysical Research* 81:1217–1230.

Sambridge M. and Gallagher K. 1993. Earthquake hypocenter location using genetic algorithms. *Bulletin of the Seismological Society of America* 83:1467–1491.

Scientific Event Alert Network. 1989. *SEAN Bulletin 14.* Washington D.C.: Smithsonian Institution. pp. 22–23.

U. S. Air Force. 2003. Archive of Department of Defense press releases, Brown P. http://www.astro.uwo.ca/~pbrown/usaf.html. October 21, 1997.

United States Committee on Extension to the Standard Atmosphere. 1976. *U.S. standard atmosphere, 1976.* Washington D.C.: U.S. Government Printing Office.

Wacker J. F., Hildebrand A. R., Brown P., Crawford D., Boslough M., Chael E., Revelle D., Doser D., Tagliaferri E., Rathbun D., Cooke D., Adcock C., and Karner J. 1998. The Juancheng and El Paso superbolides of February 15, 1997 and October 9, 1997: Preatmospheric meteoroid sizes (abstract). *Meteoritics & Planetary Science* 33:A160–A161.